
Article:
Desai, P.D., Turley, M., Robinson, R. et al. (2022) Hot microbubble injection in thin liquid film layers for ammonia separation from ammonia rich-wastewater. Chemical Engineering and Processing - Process Intensification, 180. 108693. ISSN: 0255-2701

https://doi.org/10.1016/j.cep.2021.108693

Hot Microbubble Injection in Thin Liquid Film Layers for Ammonia Separation from Ammonia Rich-Wastewater

Pratik Desai[1], Michael Turley[2], Richard Robinson[3], William B Zimmerman[4*]

1. Perlemax Ltd., 318 Broad Lane, Sheffield, S1 2LJ, United Kingdom

2.Shell Global Solutions International BV, Shell Technology Centre, Amsterdam, Grasweg 31, 1031 HW Amsterdam, The Netherlands

3.Viridor Waste Management Limited, Peninsula House, Rydon Lane, Exeter EX2 7HR, United Kingdom

4. Department of Chemical and Biological Engineering, Mappin Street, University of Sheffield, Sheffield, S1 3JD, United Kingdom

*Corresponding Author- William B Zimmerman, **email:** w.zimmerman@sheffield.ac.uk

Abstract (225 words)

With 140MT of ammonia produced per annum, over 2% of the world's total energy output is used for ammonia production. Consequently, the remediation and recovery problem is daunting. Ammonia is a pernicious pollutant with an extremely high affinity for water. Less than 2mgL^{-1} is harmful to flora and fauna but most waste streams contain between 500 mgL^{-1}-5000mgL^{-1}. Physico-chemical processes recover ammonia but are not highly effective in terms of efficiencies for such dilute solutions. Hot microbubble stripping is investigated here. It involves their injection into thin liquid layers for selective vaporization with limited sensible heating of the substrate liquid phase. The method results in several phenomena not previously observed in literature: (i) 100% separation efficiency in 30 minutes of processing time as opposed to 95% efficiency in 30 hours for the benchmark of industrial stripping; (ii) stripping of ammonia at a pH less than 9, i.e. without addition of alkaline pH modifiers and with air as a carrier gas; (iii) using cold microbubbles to strip ammonia is effective, just slower. The process is enhanced due to high mass transfer coefficients: 1000-3000 times faster than conventional stripping. This effect is explained by a new non-equilibrium chemical thermodynamics evaporation – condensation model based on Langmuir's vapour pressure prediction from the kinetic theory of gases that explains the first order kinetics, its magnitude, and the very strong temperature dependence.

1. Introduction

Ammonia removal from wastewaters has long been a subject of research interest for remediation purposes. In recent years, however, the recovery of the ammonia has become target, with the potential to produce ammonia as a co-product to the recovery – potentially profitable and sustainable. The well-known Haber-Bosch process is very effective at producing low cost ammonia, but relies on energy densities only currently achievable with fossil fuels or nuclear power. If ammonia can be recovered in an energetically inexpensive manner, CO_2 emissions are significantly reduced due to the direct reduction in emissions from recovery processes and the additional opportunistic reduction in emissions where this ammonia can replace freshly produced, i.e. recycled [1] (Desai, 2018). The recovery of ammonia is achieved by only two classes of processes: stripping and membrane separations. Ammonia stripping has recently been reviewed [1], demonstrating significant difficulty in achieving separations at pH below 9 (typically 11), with separation efficiencies higher than 90% requiring at least 4 hours processing time, including those with membrane components, with the single exception of microwave intensification of stripping, which achieved 94.2% separation efficiency in 1 minute of processing time, albeit with 750W of power for 750mL of volume treated [3]. Upscaling microwave intensification of most processes is problematic, but the energetics are also challenging.

One very promising aspect of ammonia recovery from wastewaters is the potential to operate anaerobic digestion for the continuous production of ammonia. Nguyen [4] used process simulation to demonstrate the feasibility of continuous ammonia stripping from anaerobic digestion (AD), using the workhorse ADM1 model accepted as representative for AD operations. Riaño et al. [5] demonstrated experimentally that semi-continuous operation with swine manure is achievable, using gas permeable membranes. This follows on from the demonstration with conventional batch AD operation with the same feedstock, recovering 96-98% of the ammoniacal nitrogen content in 5 days with aeration, against the control of 25 days without aeration [6]. They estimated a 70% reduction in ammonia treatment costs using low-level aeration for the gas permeable membrane stripping.

Recent advances in gas permeable membrane harvesting of ammonia are heralded by Lee et al. [7], where pH 9 operation achieved a mass transfer coefficient of 0.216 h^{-1}, while pH 11 operation achieved 0.324 h^{-1}, treating a real wastewater with characterized ammoniacal nitrogen composition. These are comparable with stripping technologies reviewed by [2] with the exception of rotating packed bed reactors (12.3 h^{-1}) and microwave intensification (3.35 h^{-1}) which are clearly much higher in power density consumption. Lee et al. [7], however, clarifies the major reason that none of these technologies have yet been adopted for industrial wastewater treatment and ammonia harvesting – the dissociation of ammonia in aqueous solution (equation 1) must be counteracted by the Le Chatelier's principle "push" of high alkalinity (boosting hydroxide ion concentration), yet still achieves poorer performance (long processing times / slower mass transfer rates) than destructive classes of ammonia wastewater treatment – oxidation, absorption, and chemical precipitation – which are in widespread use.

$$NH_4^+ + OH^- \leftrightarrow NH_3 + H_2O \qquad (1)$$

For a basis of comparison, membrane separations are widely adopted in ethanol-water separations, so called molecular sieves, for dehydration from the azeotrope, to meet biofuel purity requirements [8]. Ethanol does not dissociate to an appreciable extent in aqueous solutions, including fermentation broths. In some sense, ammonia recovery should be viewed as a reactive separation because the equilibrium re-association reaction (1) must be achieved, similar to conventional gas-liquid catalytic reactors [9].

The purpose of this paper is to explore the efficacy of part of stripping without the gas permeable membranes, but with hot microbubbles. The evaporation and condensation dynamics of hot microbubbles was first studied by [10][11], with the remarkable feature that the internal composition of, say, 200 μm diameter bubbles achieve internal homogeneity and chemical equilibrium with the microbubble interface in time scales of just a few milliseconds, but can maintain much higher temperatures than the surrounding liquid. This latter feature follows from microbubbles generated by fluidic oscillation being injected in, and maintaining, laminar flow. Laminar thermal boundary layers are highly resistant to bulk heat transfer. This combination of features results in the rapid humidification of the vapour phase when the contact time (controllable by gas injection rates and the

liquid layer height) is limited to milliseconds before the microbubbles burst. It is an essentially non-equilibrium phenomenon since the thermal driving force is maintained to be very high. This approach achieved azeotrope breaking [8][12] as well as high partition coefficients [13].

The analogous hypothesis posited here is that one can use the concentration gradient in the bubble (the air bubble has zero ammonia concentration whilst the surrounding liquid has a higher ammonia concentration) and the associated temperature gradient (difference of the injected air bubble temperature and liquid temperature) to speed up the concentration gradient effect via the Soret effect [14]. The hot air microbubble is injected with zero ammonia concentration in the gas phase initially. Subsequent mass transfer occurs due to the combination of temperature based gradient phase separation and concentration based gradient observed in this work. Because only ammonia molecules can be removed by the bubble phase, not ammonium ions, microbubble stripping provides a Le Chatelier's principle "pull" on the dissociation reaction (1), potentially relieving the requirement for alkaline pH "push". This happens, hypothetically, until reaching steady state where, the dissolution rate of already stripped ammonia on the microbubble balances the stripping flux. The rate of transfer is determined by the contact time of the bubble with the substrate liquid, *i.e.* by liquid layer height (the most simple tuning parameter).

The paper is organized as follows. In Section 2, Methods and Materials are presented, notably the use of fluidic oscillation to inject microbubbles into a test cell purpose designed to control liquid layer height initially. Section 3 describes the results while discussing and analysing their significance, especially the characterization of mass transfer rates. The conclusions are drawn the final section.

2. Method and Materials

2.1 Fluidic oscillation induced microbubbles

A jet diversion fluidic oscillator (FO) of the type described in [15-20] has been used. Bubble sizes between 70 μm -150μm (volume average bubble size) have been obtained with FO-sparger combination [21] measured using methods seen in Desai et al. [22].

2.2 Pneumatic set up

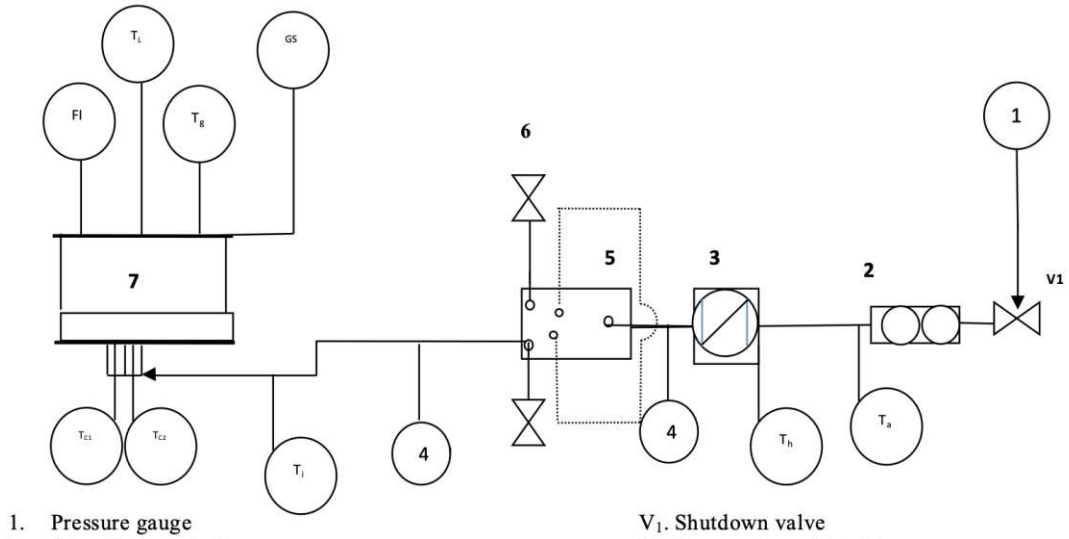

1. Pressure gauge
2. Mass flow controller
3. Process air heater
4. Pressure transducer – before and after fluidic oscillator
5. Fluidic oscillator
6. Venting valves
7. Microbubble generating unit

V_1. Shutdown valve
T_L Temperature of liquid
T_g Temperature of off gas
T_c Temperature of chambre
T_i Temperature of inlet
T_h Temperature of heater
T_a Temperature of ambient air
GS Gas sensor- ammonia

Figure 1 System Schematic

The system design follows the precepts of hot microbubble stripping used by [8][10][12][13]. The test cell is a single unit of the microbubble stripper, labelled unit 5 in the system schematic shown in Figure 1. The ammonium hydroxide solution is placed inside this test cell. The air supply is regulated via a pressure gauge and into an emergency shut down valve (V1 – standard ball valve). This is followed by a mass flow controller (GFC17) which is used to control the air flow rate into the test cell. The temperature at this point is noted using a thermocouple. This is then fed into a process air heater (750W) which then heats the air to the required temperature (the heater temperature is measured and the control thermocouple is placed in the chambre of test cell). Process air heater is controlled using a PID controller with measurement for the control thermocouple being in the chambre right beneath the sparger. The pressure of the system is measured (for room temperature (25ºC) air, using Impress G1000 Pressure Transducers), and the controlled air flows into the fluidic oscillator following the heater. Appropriate amount of air is then siphoned off into the test cell as determined by the flow rate requirements of the oscillator. The inlet is split into a trident to equalise the flow and a pair of equi-

responsive thermocouples assist in temperature control, allowing the monitoring for even flow distribution, and acting as redundancies for safety purposes as the sparger requires to be at a low pressure drop (to reduce operational costs) and have equal flow across the sparger. A flow indicator, gas sensor, and sets of thermocouples maintained at different liquid heights measure temperature for given liquid depth are additional measurements. An off gas thermocouple is also present. The sparger is a sintered steel membrane of 100μm pore size, with a 30 mbar pressure drop as the bubbling pressure, with an area of 150x30 mm^2. The height of the liquid above the membrane is correlated with the volume poured in over the active area. It should be noted that there is no back pressure issue during operation as the air flow is on with a sufficiently low level to oppose imbibition into the microporous diffuser while the solution is added to the test cell. Offgas from a top port on the test cell is vented to the fume cupboard so that pressure does not build up.

2.3 Chemicals and Chemical Analysis

Table 1 shows the design of experiments conditions for which combinations are selected to explore the parameter space using factorial methods.

2.3.1 Ammonia Solution

Standard ammonia solution was prepared using dilution of ammonium hydroxide, Fischer Scientific, 7732-18-5 for analysis, 20% ammonium hydroxide solutions and they were diluted appropriately and checked with 1000 ppm (0.1M) standard – Cole Parmer (Item#WZ-27503-00)

2.3.2 Ammoniacal nitrogen concentration

The ammonium concentration in the solution was directly measured using the Cole-Parmer ammonium ion selective electrode (ISE) (#WZ-27504-00) as per the American Public Health Association (APHA) Standard Method for the examination of water and wastewater [23] and literature [24-28]. The probe can operate up to 18,000 ppm (~18,000 mg/L). Special low level calibration is recommended for less 1.0×10^{-5} M (0.18 ppm as ammonium) solutions. The lowest detection limit is 0.01ppm, indicating typical operation allows for up to 6 orders of magnitude of precision in the normal calibration mode. It should be noted that continuous measurement for the liquid ammoniacal nitrogen composition is not

possible due to the delay time for the membrane to work. The 5mm liquid layer height is eventually adopted as the lowest practicable leel so that it would not be affected by potential incongruences, specifically imbibition into the pores, in the cell, opposing repeatability of the experiments.

2.3.3 pH

The pH of the solution was directly measured using a Mettler Toledo LE 409 pH probe.

Table 1: Experimental Design

Variable	-	+	Basis
Temperature (°C)	80	140	The temperature was chosen to be the same as that used where vaporisation of water was also explored [10].
Initial pH	10	11.5	Srinath and Loehr [29] suggested that, at a pH = 10.0 and T = 20 °C (room temperature), the fraction of undissociated ammonia is 0.796 and for pH = 11.5 and T = 20 °C, 0.975. Therefore, this experiment should show the effect, if any, of this difference and if evaporation of the water or removal of ammonia pushes equilibrium towards further production of ammonia without additional alkali [30].
Depth of liquid (mm)	3	15	The depth of liquid was chosen to be the minimum used -3 mm. The maximum height to be used is limited by the height of the experimental vessel.
Time (hrs)	0.5	1	The time was chosen to be 0.5 - 1 hours as this is well within the target operating envelope
Initial concentration (mg L^{-1})	500	2000	Initial concentrations of 500 mgL^{-1} - 2,000 mgL^{-1} were chosen as wastewater which have been stripped in literature have typically had concentrations within this range
Air flowrate (LPM)	1	2	Rated flow across the designed sparger.
Liquid Temperature (°C)	20	35	Wastewater (major source of ammonia) would be at a higher temperature.

2.4 Design of experiments

A quarter factorial design of experiments were conducted according to the experimental design in Table 1 as a preliminary set of experiments to scope the first six parameters, which were identified as the most likely to be controlling. As a point of clarification on Table 1, the liquid and air temperatures are initially different and maintain substantial difference in temperature, which is a feature of hot microbubble stripping [8][10-13] as the non-equilibrium thermal driving force accelerates evaporation. From these 16 scoping experiments, it was determined that liquid layer height had the strongest sensitivity, and best performance was achieved with the lower (-) liquid height of 5mm, which is the lowest level for which control is easily possible. [8][10][12][13] found best performance with 1mm

liquid level in those experiments, but relied on vapour phase sensors to assess performance. As the ammonium ion probe must be submerged in the liquid, 5mm depth for the initial condition achieves this. The highest removal rates of ammonia in the scoping studies (>99%) occurred with liquid layer height 5mm, air flow rate 2LPM, and duration of processing at 30min, so these values were set as the "defaults" for the experimental results reported in Section 3. Hence variation of air temperature and initial pH are the major variables studied extensively in Section 3.

A major surprise from the scoping study was that the dependence on initial concentration of ammonia in the aqueous solution was the least sensitive of the six parameters studied. To an excellent approximation, the removal efficiency is independent of initial ammonia concentration, indicating a first order rate process in ammonia. From this perspective, the default ammonia concentration was set to 2000 ppm (+ in Table 1), as it is the easier solution to produce. Given the detection limit in the normal calibration of 0.18 ppm, this ensures 5 orders of magnitude precision is possible, should removal efficiencies approach, as desired, 100%.

It should be noted that the maximum liquid volume used in the test cell is found from the highest operable liquid layer height (15mm) multiplying the sparger planform area, 150x30 mm^2., i.e. 67.5ml. The default volume taken is 22.5ml. The appropriate scaling parameter for gas sparging is reported as vvm, the volumetric flow rate test cell liquid volume divided by with per minute time units [31], so the default vvm is 89 min^{-1} in Section 3. For classification purposes, the study conducted here is a batch separator, with no liquid throughput, and thus inherently transient. The next subsection describes the adaptation of the conventional data analysis for such systems.

2.5 Transient Mass Balance Data Analysis

Ammonia preferentially disappears from the liquid phase in the test cell due to the evaporation mediated by hot microbubble stripping. Since ammonium ion selective probe is immersed in the liquid phase, a component mass balance on ammoniacal nitrogen can be conducted.

$$Accumulation = In - Out + Generated - Reacted$$

$$\frac{dC}{dt} = -kA_iCF \quad (2)$$

Where: C = concentration of ammoniacal nitrogen (mol)
k = mass transfer coefficient (m^{-2} h^{-1})
F = fraction of undissociated ammonia
A_i = interfacial area (m^2)

F is given by:

$$F = \frac{10^{pH}}{\frac{k_b}{k_w}+10^{pH}} \quad (3)$$

Substituting (3) into (2) yields:

$$\frac{1}{C}dC = -K_D\left[\frac{10^{pH}}{\frac{k_b}{k_w}+10^{pH}}\right]dt \quad (4)$$

Where K_D = overall mass transfer coefficient, kA_i (h^{-1})

In this experiment, pH is uncontrolled and so decreases linearly with time such that:

$$pH = pH_0 - zt \quad (5)$$

Where: $z = (pH_0 - pH_1) /(t_1 - t_2)$

Substituting (5) into (4) and integrating:

$$\ln\left[\frac{C_2}{C_1}\right] = \frac{K_D}{z\ln[10]}\left(\ln\left[\frac{k_b}{k_w}+10^{pH_2}\right] - \ln\left[\frac{k_b}{k_w}+10^{pH_1}\right]\right) \quad (6)$$

Denoting $\frac{k_b}{k_w}+10^{pH_n}$ as L_n:

$$\ln\left[\frac{C_2}{C_1}\right] = \frac{K_D}{\ln[10]}\frac{(t_2-t_1)(L_2-L_1)}{(pH_1-pH_2)} \quad (7)$$

Equation (7) is derived by Srinath and Loehr [29], however, it is noted that they carried an error forward by integrating (4) to give an equation which proscribes pH as rising with time. Defining efficiency, η, as:

$$\eta = \frac{C_1 - C_2}{C_1} \times 100\%$$

Equation (7) can be rearranged to give:

$$\eta = 100\left(1 - e^{\left(\frac{K_D\ (t_2 - t_1)(L_2 - L_1)}{\ln[10]\ \ (pH_1 - pH_2)}\right)}\right) \quad (8)$$

Srinath and Loehr [29] define k_b / k_w as:

$$\frac{k_b}{k_w} = (-3.398 \ln[0.0241 \times \theta(°\mathrm{C})]) \times 10^9 \quad (9)$$

Therefore, the non-linear regression curve takes the form:

$$\eta = 100\left(1 - Ae^{(BT_{air,inlet})}\right) \quad (10)$$

Where *A* and *B* are constants which are fitted by nonlinear least squares regression to be -57.53 and 0.02374 respectively. The resulting curve closely follows the data, justifying crediting the inlet air temperature for the efficiency, rather than the liquid temperature which is transient and therefore more complicated to correlate with efficiency. Using the constants, the overall mass transfer coefficient, K_D, can be found by from (8) and (10).

3. Results and Discussion

A parametric study was carried out using the experimental design window parameters as the boundary conditions in order to better understand the underlying mechanism for the system and quantify the mass transfer information.

3.1 Parametric trials

The parameters used for this trial were temperature of the inlet air, initial ammonia concentration, pH of the system, and mapped against the processing time. Those studies that show error bars on the associated graphs were conducted in triplicate.

3.1.1 Temperature Trials

Temperature studies for air inlet temperature were conducted from 22ºC onwards to 140ºC. The air temperature could be high with the liquid temperature remaining lower at about 30ºC -50ºC due to very

little sensible heating taking place. Figure 2 shows the efficiency of the process with a variety of inlet air temperatures.

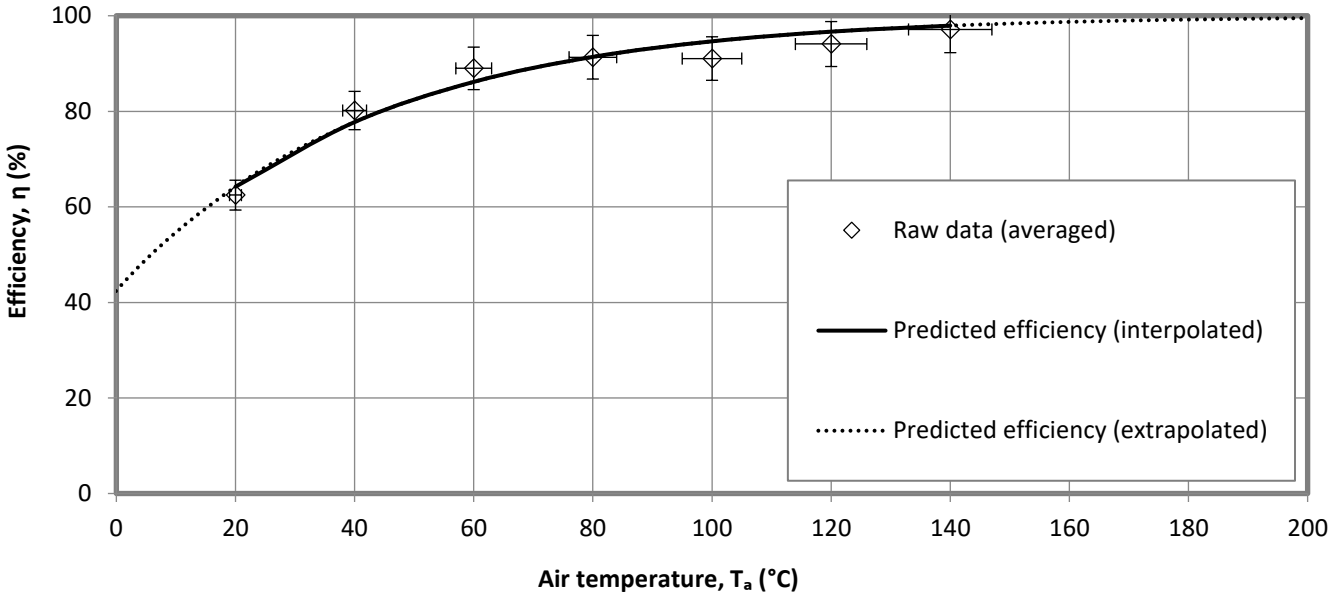

Figure 2 Efficiencies for a range of inlet air temperatures. The non-linear regression line of best fit is plotted across the data and extrapolated. The error bars created using the data from the averaged runs of each inlet air temperature. The run time was fixed at 30 minutes.

Upon conducting the ammonia mass balance according to Section 2.4, the resulting values are reported across the range of temperatures in Figure 2. The figure shows an excellent correlation ($R^2 = 0.9996$) between the inlet air temperature (rather than transient) and the coefficient thereby justifying the use of the average liquid temperature to determine L_n. The stark feature is that they agree on K_D with ~10^1 magnitude. Srinath and Loehr [29] reported $K_D \sim 10^{-3}$ magnitude whilst Smith and Arab [32] as between 10^{-3} and 10^{-2}. This can be explained by noting that the size of the fine bubbles typically used in literature are of a millimetre scale. This increase and further improvements are due to the substantially increased surface area *wrt* volume. There is also the thin layer effect for the boundary and the high internal mixing within the microbubble as shown in [10][12].

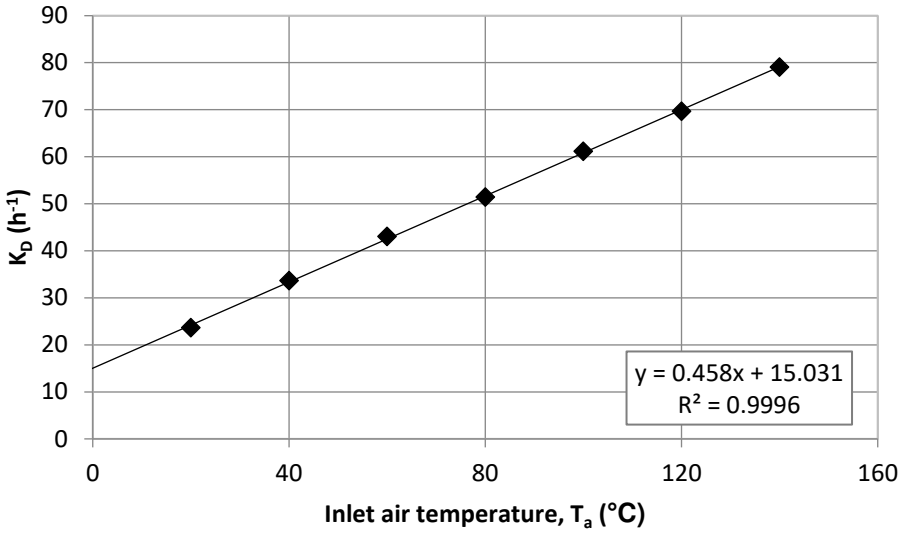

Figure 3. Overall mass transfer coefficient vs. inlet air temperature with a linear regression and the corresponding correlation and equation for the 30 minute run.

Figure 4 shows the average liquid temperature curve for various temporal runs. This shows that the liquid temperature does not rise significantly even at an inlet air temperature of 180ºC. Different layer heights are shown as although layer height reduction results in an increase in efficiency, there is a decrease in the throughput observed.

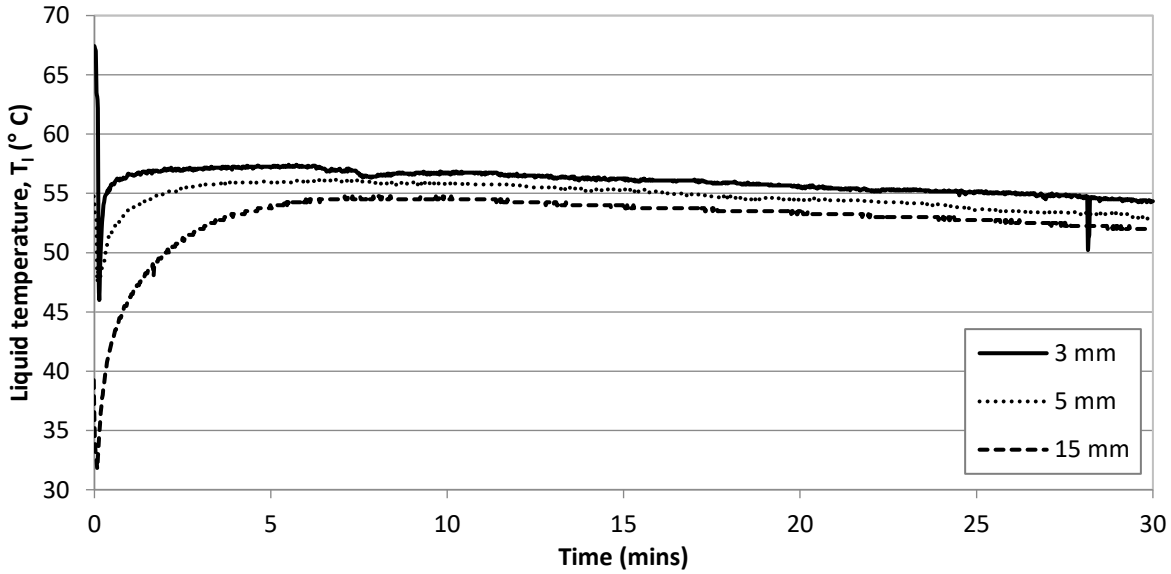

Figure 4 Liquid temperature over time and an average of the 3 runs for each liquid height using thermocouples placed at different locations.

The initial immediate drop has been included to show the sharp decrease in temperature when the liquid enters the vessel. This is for air temperature at 180ºC and for a 30 minute run – higher temperature used in order to test whether liquid temperature would concomitantly increase.

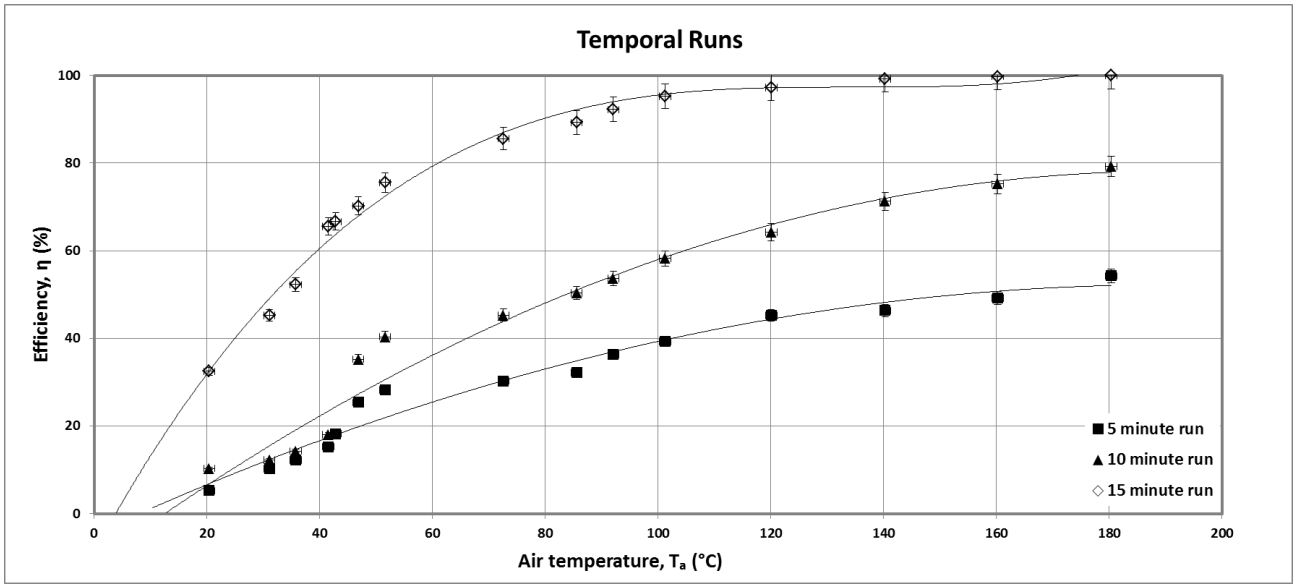

Figure 5 Temporal run carried out in order to see the efficiency for various temperatures.

Figure 5 compares various inlet air temperatures with a temporal run in order to demonstrate that whilst 30 minute runs seen in Figure 2 show high stripping efficiency, there is an advantage to run the system at the 15 minute run if inexpensive process-heat is available as similar stripping efficiencies are achieved with lower CAPEX/OPEX ramifications.

There is an observable decrease in performance when concentration basis is used instead of total mass for the ammonia. This is because there is a competing process – dewatering – over ammonia stripping which is exacerbated for lower liquid heights across the membrane. According to experiments with a selected condition fixing all other parameters allowing just variation of the liquid layer height, a difference in performance is observed. For a lower layer height, there is volume reduction in total liquid observed. The dewatering step is also hastened due to this and we have observed a dramatic increase in mass transfer when using lower liquid heights such as [8][10][12][13]. This results in a significant reduction in the total liquid volume which then results in a ‘lower’ efficiency of ammonia removal and

an increase in concentration of ammonia. This is easily rectified by adding a partial condenser for the evolving vapours which will ensure that the water re-enters the system whilst ammonia remains as a gas and escapes the system. However, Figure 6 demonstrates the effect for two points in the trial. The total ammonia removed is still high (which is seen in the mass basis) and the volume reduction decreases (as the bubble gets wetter with therefore the concentration difference reduces) with increased layer height. It is observed that the liquid layer height increase results in higher efficiencies as compared to what has been observed previously in literature. The mass basis demonstrates the performance better. The negative percentage simply means that the dewatering process is taking place at a higher rate and this can be negated by placing a condenser to condense the liquid back into the solution.

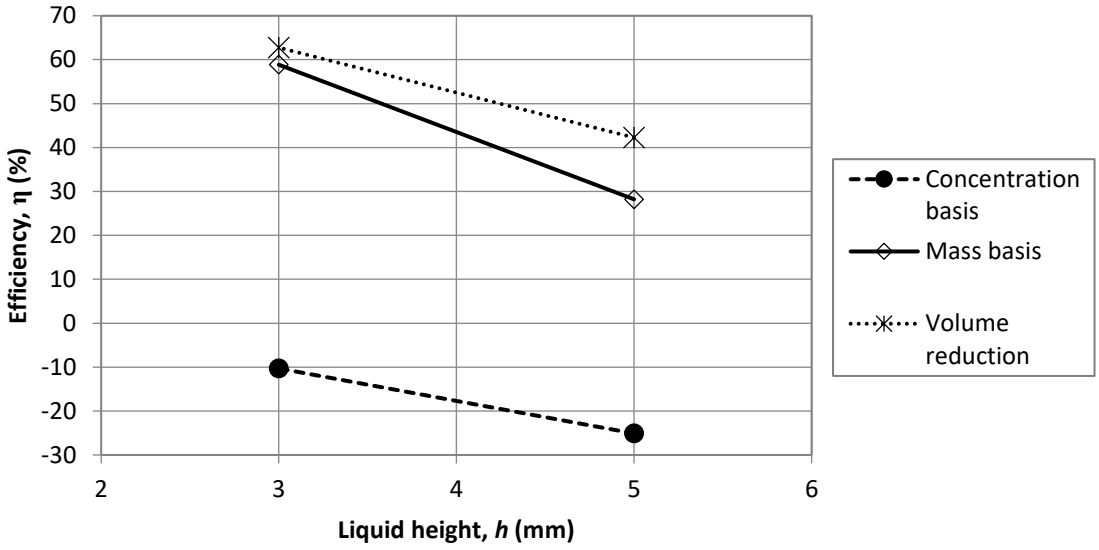

Figure 6 Ammoniacal nitrogen removal on both mass and concentration bases with percentage volume reduction plotted.

pH variation was also explored. Concentration and mass basis were used to calculate removal efficiencies. Figure 7 and Figure 8 show the pH study.

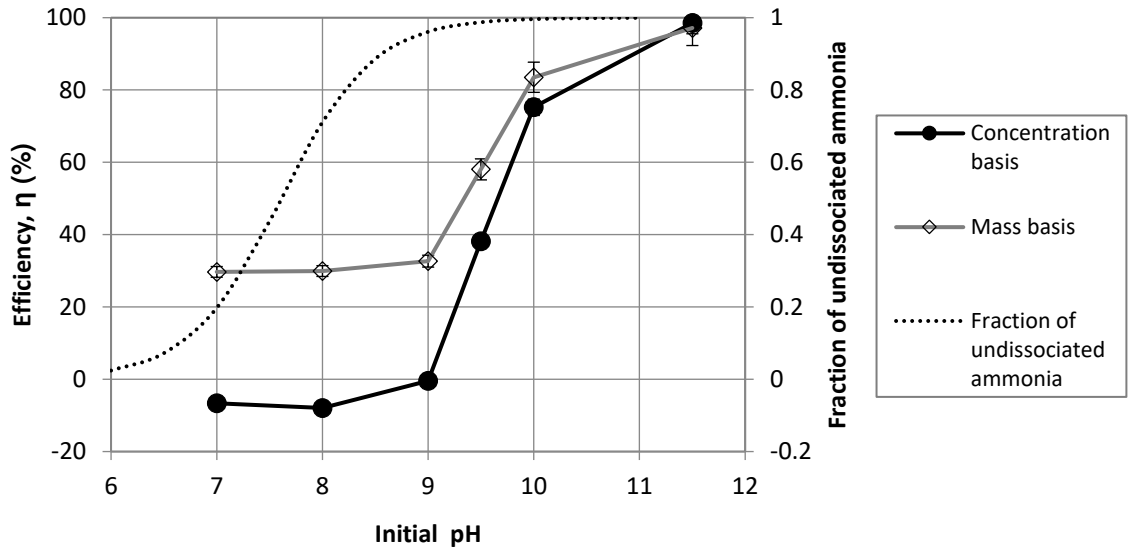

Figure 7 Average efficiencies on both mass and concentration bases with the theoretical fraction of un-dissociated ammonia also plotted [33]. 30 minute run with 140ºC air temperature. Error bars cannot be seen in the figure, but are less than 3%.

Higher pH will increase the stripping efficiency significantly and agrees well with literature. However, the ability to strip ammonia even at a pH lower than 7 has not been observed in literature while it has been achieved here. This is due to the dewatering step which forces the ammonia out of the solution and the rate of reaction mitigates recombination that forms the ammonium hydroxide. Increasing the pH creates a strong concentration gradient. According to Le Chatelier's principle, the presence of the OH^- favours re-association of ammonia, thereby increasing the ability to strip ammonia out. Raising the pH for the same experiment between 8 to 10 increases stripping performance significantly from 30% removal efficiency to 87% in terms of concentration and from 60% in terms of mass to 92%. This is observed in Figure 8. Alternatively, the microbubble stripping efficiency can be increased to 95% without pH change by extending processing time to 1 hour.

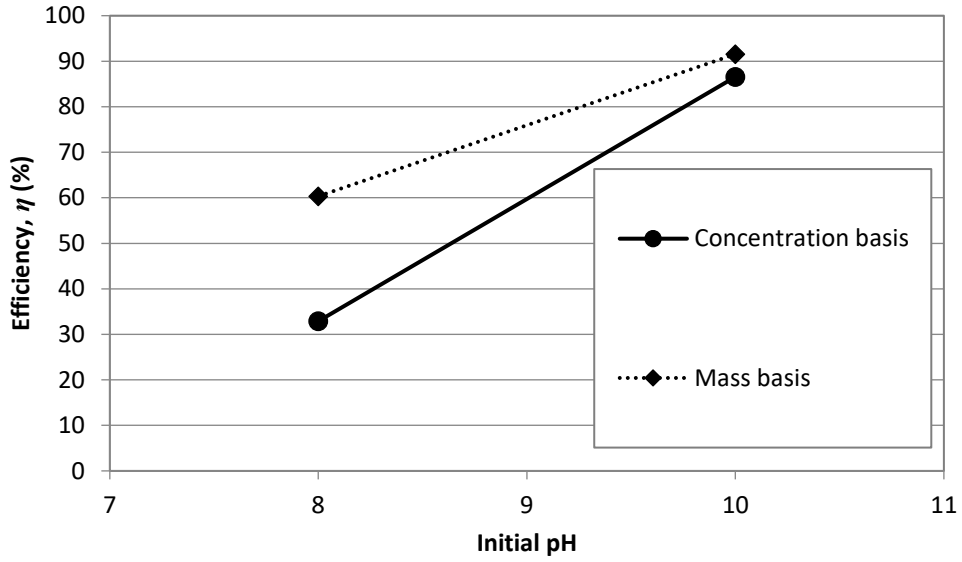

Figure 8 Removal efficiencies for ammonia.

The difference in separation efficiencies can be seen for the mass and concentration basis in Figure 8. However, the difference is greater for lower pH as compared to the higher pH. This is due to the fact that the processes of dewatering and stripping are competitive and the increase in pH results in an increased gradient thereby improving the ability for the ammonia stripping to take place.

The mechanism for enhanced removal efficiency has to do with competing vaporization and condensation processes. Abdulrazzaq *et al.* [12] introduced an evaporation-condensation model, which is for highly non-equilibrium driving forces in the microbubble phase, which holds in the few milliseconds of contact time:

$$\dot{n}_i = k_i A(x_i \gamma_i P_i^* - P_i) \qquad (11)$$

The LHS of (11) is the molar exchange rate of species i (ammonia and water); k_i is the component Langmuir-type collision coefficient; A is the surface area of the microbubble phase; x_i is the mole fraction of the species in the liquid phase; γ_i is the activity coefficient; $P^*_i(T_g)$ is the saturation pressure at the temperature in the microbubble phase; P_i is the partial pressure in the microbubble phase. The RHS of (11) , if set to zero (equivalent to no net exchange of species across the microbubble interface), is the generalized Raoult Law. Hence, the driver for mass transfer is the difference from equality of the Raoult terms. Commonly, the approach to equilibrium at gas-liquid interfaces is so rapid, equilibrium

is assumed to hold. However, hot microbubble stripping is an inherently transient process, with the contact time of any single microbubble engineered to be a few milliseconds, so an evaporation-condensation non-equilibrium rate law holds. The microbubble has so little time for heat transfer through the laminar boundary layer, that it can only exchange heat (and mass) with the microbubble interface. This maintains the high thermal gradient. Similarly, microbubbles enter with no ammonia or water vapour, so has a strong chemical thermodynamic driving force -- $P_i = 0$ upon injection – so the driving force on the RHS of (11) is maximal.

Equation (11) is the form of de Donder's chemical affinity [34], later popularised by Prigogine [35], that shows for the first molecule of product initially entering the microbubble phase, Gibbs free energy is effectively infinite, overcoming even highly endergonic reaction system, *e.g.* the re-association of ammonium and hydroxide ions, in this case.

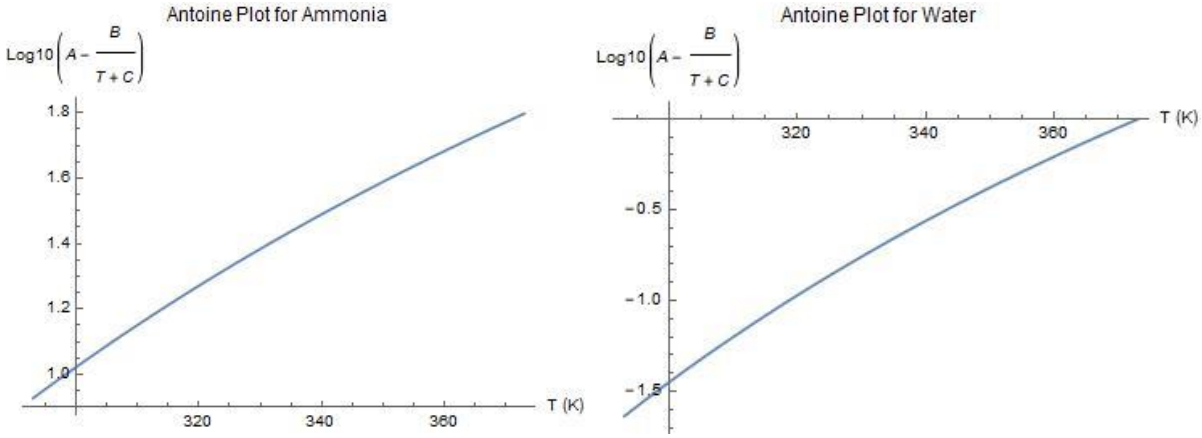

Figure 9 Antoine Plots for Ammonia and Water over the temperature range [293K, 373K], where the ordinate in $\text{Log}_{10}(P^*_i)$ with in P^*_i bars. The plots are nearly linear, with the $\Delta\text{Log}_{10}\text{P}$ ~1 for ammonia and $\Delta\text{Log}_{10}\text{P}$ ~1.8 for water over that range.

Generally, saturation vapour pressure is only considered for liquids below their boiling points. But vapour pressure above a liquid exists in a header space with any temperature above its boiling point. Stull[98] experimentally determined such vapour pressures over ranges of temperatures for many volatiles below and above their boiling points, including ammonia and water. Figure 9 shows the Antoine plots for Stull's data for ammonia and water [36]. NIST computed the Antoine coefficients from Stull's data, but Figure 9 does not depend on the coefficients of best fit.

There are two important observations from Figure 9 – water actually increases in $P^*(T_g)$ more rapidly than ammonia in this range, but ammonia's $P^*(T_g)$ is very large (~9-90 bar), so the RHS of (11) is always large. Consequently, the rate of ammonia evaporation is practically independent of the partial pressure of ammonia in the microbubble phase, and therefore (11) is a first order rate law in the mole fraction x of ammonia, with the rate constant strongly temperature dependent (Figure 3). These predictions are in complete agreement with the observed temperature dependency of the removal efficiency, and the observation that the removal efficiency is independent of initial liquid concentration of ammonia – consistent with the first order process demonstrated phenomenologically in Figure 3.

This theory also explains the observed difference in removal efficiencies of ammonia on mass basis and on a concentration basis, where concentration removal efficiency "underperforms" in Figure 6 at all levels of pH, and even has a negative efficiency regime for concentration. The competing removal of water to ammonia has an advantage that water can vaporise directly, whereas the ammonium and hydroxide ions must re-associate to molecular ammonia to be vaporized. The Gibbs free energy cost of the ammonia re-association reaction is not included in (11), but is clearly pH dependent. However, at high enough alkalinity, it is no longer a barrier. With sufficiently high temperature, the Gibbs free energy released according to (11) overcomes this additional re-association barrier (even at lower pH) and is then a first order kinetics process.

Figure 10 places the performance of the best and reproducible hot microbubble stripping experiment demonstrated by temperature variation in Figure 2 (100% removal in 15 minutes, up to the ammonium probe precision of four significant figures) into the context of the literature on industrial performance of the four classes of ammonia removal stripping, adsorption, chemical precipitation, and oxidation. Kinidi et al. [2] reviews more promising technologies from the lab bench which also achieve in the target green box of Figure 10 (not included), while tabulating the mass transfer coefficients. The best of these lab bench technologies, a rotating packed bed reactor, has just half the mass transfer coefficient of microbubble stripping at room temperature (cf. Figure 3), further only 6.4-fold less than hot microbubble stripping mass transfer coefficient at 140ºC injected air temperature, while only achieving 64% recovery.

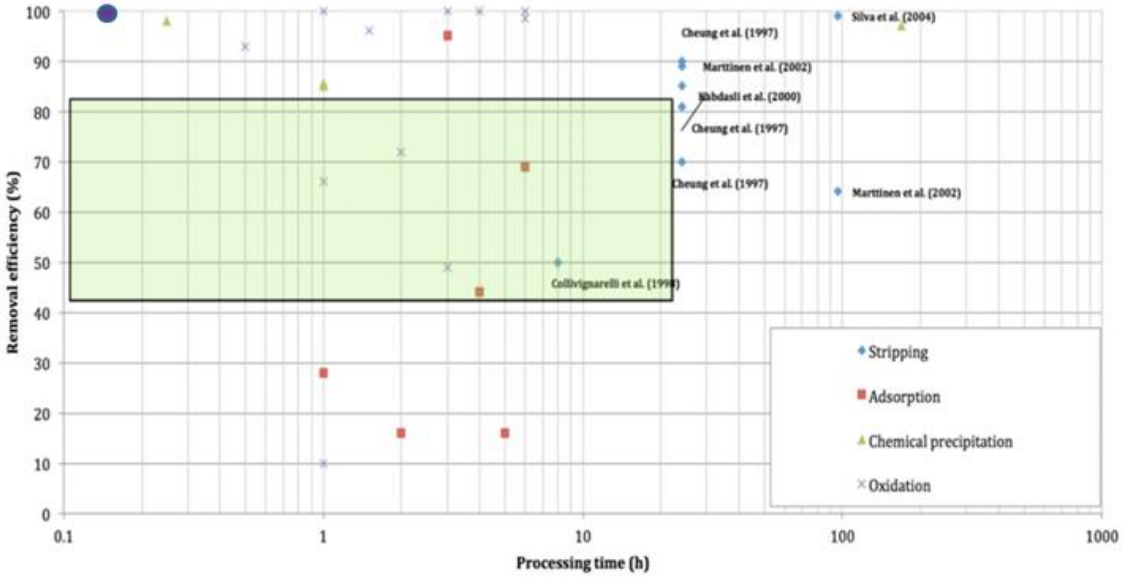

Figure 10 Large dot is the best performance found in Figure 2 shown relative to the conventional industrial processes of stripping, adsorption, chemical precipitation, and oxidation. (Table containing data points in supplementary information). The green box delineates what would be an appropriate operating regime– processing time within 24 hours and removal efficiencies from 50- 100%).The versatility of the designed process ensures that several routes can be used in order to get similar performances based on availability and requirements and driving forces- sustainability, energetics, availability of process heat being some examples.

Table 2 Kinidi et al. [2] Summary of Recent Ammonia Stripping Intensification Processes

Ammonia stripping processes	Aqueous solution volume	Removal effectiveness (%)	Stripping time (h)	Airflow rate	Mass transfer coefficient (h^{-1})
Packed tower	1000L	75	3.5	25 (air to liquid ratio)	0.42
Semibatch jet loop reactor	9 L	97	5.8	5.6 (air to liquid ratio)	0.63
Water-sparged aerocyclone	10 L	98	3.5	11.4 (air to liquid ratio)	1.2
Rotating packed bed reactor	0.025–0.01 L/min	64	0.0037	1800 L/min (continuous flow)	12.3
Membrane contactor	0.94 L	99.83	10	Not available	0.011
Membrane distillation	1 L	98.5	4	Not available	0.079
Ion exchange loopstripping	2 L	84.6	2.5	Not available	Not available
Microwave radiation	0.75 L	94.2	0.0167	10 (air to liquid ratio)	3.354
Hot microbubble stripping†	0.0675L	99.999	0.5	2 L/min	79.2

This study, Figure 3, initial air temperature 140°C.

Table 2 reports the comparison of the 8 stripping studies reviewed by Kinidi et al. [2] with the top mass transfer coefficient reported here for hot microbubble stripping. Clearly this table is insufficient information to assess process economics, which requires a full process simulation with sufficiently high technology readiness to estimate industrial scale performance with optimized design for equipment and operating costs. Energetics and process integration are important issues, but hot microbubble stripping can operate with waste heat of 40°C with 79% recovery according to Figure 3, so certainly integrates well with many wastewater treatment plants with higher temperatures generated by the operation of air blowers, as observed by the authors on plant visits. Whether any of these process intensified technologies reported in [2] upscales to industrial field scale is uncertain, but the authors are aware that hot microbubble stripping has passed pilot scale trials with even better performance than the lab bench trials reported here, on ammonia recovery from industrial wastewaters.

4. Conclusions

The promise of this study is the scope to recover the ammonia *in situ*. A non-equilibrium chemical thermodynamics evaporation – condensation model is proposed based on Langmuir's vapour pressure prediction from the kinetic theory of gases (*cf.*[12]). It is applied here for the first time to a volatile species *above* its boiling point, providing a first order kinetics theory consistent with the observed, phenomenological first order mass transfer dynamics of ammonia removal by hot microbubble stripping. The strong temperature dependence has its explanation in the large chemical non-equilibrium driving force of ammonia vapour pressure at saturation. The first order behaviour for ammonia removal is essential for its treatment of dilute solutions, so pernicious to aquatic flora and fauna.

The process has the potential for widespread impact on ammonia-rich wastewater remediation: the possibility to treat to the ammonia liability while providing a possible value stream (raw ammonia source) instead of destroying the ammonia. Ammoniacal pollution is a worldwide problem and this paper identifies an encouraging route for a circular economy approach to solving this challenging problem.

1000-3000 times increase in mass transfer coefficient for ammonia stripping has been observed, relative to adopted *industrial* stripping of ammonia from wastewaters.

Ability to strip ammonia at pH lower than 7 due to vaporisation being the chief driving force and not concentration gradient.

This process is potentially a supplemental approach for generating sustainably sourced ammonia. The rate of ammonia recovery and the versatility of the process results in several possibilities and converts conventional liabilities related to ammonia-rich wastewater streams into revenue generating streams. The process can simultaneously be used to reduce, *in situ*, ammonia related inhibition of anaerobic digestion, thereby increasing capital efficiencies of anaerobic digesters without substantial changes in CAPEX/OPEX [37] for the "re-purposing" of the anaerobic digester as a potential *sustainable* source of ammonia. This process has been designated as Microbubble Stripping as it is analogous to conventional air stripping.

Acknowledgements

This work was carried out as part of the "4CU" programme grant, aimed at sustainable conversion of carbon dioxide into fuels, led by The University of Sheffield and carried out in collaboration with The University of Manchester, Queens University Belfast and University College London. The authors acknowledge gratefully the Engineering and Physical Sciences Research Council (EPSRC) for supporting this work financially (Grant no. EP/K001329/1). The authors would also like to acknowledge the support provided by Elliot Gunard and Andrew "Andy" Patrick from the technical workshop at the Department of Chemical & Biological Engineering, University of Sheffield. Pratik Desai would like to thank G. Knowles for inspiration. Pratik Desai would also like to thank Pascaline Verrier and Edouard Baril for bias prevention studies. Pratik Desai would also like to thank Marcus Thomas from Viridor and ALS Environmental for their support in the study.

References

[1] P. Desai, *Waste Factory - Microbubble Mediated Ammonia Recovery Processes - MMARP In:* Dubey, B., ed. 13th World Congress on Biopolymers and Bioplastics and World Congress on Recycling August 28-30 2018 2018 Berlin, Germany. Expert Opinion on Environmental Biology. DOI: 10.4172/2325-9655-C5-031, 2018.

[2] L. Kinidi, I. Ai Wei Tan, N. Binti Abdul Wahab, K . Fikri Bin Tamrin , C. Nolasco Hipolito, S. Faridah Salleh. Recent Development in Ammonia Stripping Process for Industrial Wastewater Treatment, *Int. J. Chem. Eng.* 3181087, 2018.

[3] O. N. Ata, K. Aygun, H. Okur, A. Kanca, "Determination of ammonia removal from aqueous solution and volumetric mass transfer coefficient by microave-assisted air stripping," *International Journal of Science and Technology*, 13(10): 2459–2466, 2016.

[4] H.H. Nguyen, Modelling of Food Waste Digestion Using ADM1 Integrated with Aspen Plus. *PhD thesis*, University of Southampton, 2014.

[5] B. Riaño, B. Molinuevo-Salces, M.B. Vanotti, M.C. García-González, Application of Gas-Permeable Membranes For-Semi-Continuous Ammonia Recovery from Swine Manure *Environments 6*:32, 2019.

[6] P.J. Dube, M.B.Vanotti, A.A. Szogi, M.C. García-González, Enhancing recovery of ammonia from swine manure anaerobic digester effluent using gas-permeable membrane technology, Waste Management 49: 372–377, 2016.

[7] W. Lee, S. An, Y. Choi, Ammonia harvesting via membrane gas extraction at moderately alkaline pH: A step toward net-profitable nitrogen recovery from domestic wastewater, *Chemical Engineering Journal* 405, 126662, 2021.

[8] N. Abdulrazzaq, B. Al-Sabbagh, J.M.Rees, W. B. Zimmerman, "Separation of azeotropic mixtures using air microbubbles generated by fluidic oscillation", AICHEJ DOI: 10.1002/aic.15097 (2015).

[9] SK Kurt, F Warnebold, KDP Nigam, N Kockmann, Gas-liquid reaction and mass transfer in microstructured coiled flow inverter, Chemical Engineering Science 169, 164-178, 2017.

[10] W.B. Zimmerman, M.K.H. Al-Mashhadani, H.C.H. Bandulasena, "Evaporation dynamics of microbubbles", Chemical Engineering Science, 101:865-877, 2013.

[11] W.B. Zimmerman, Towards a microbubble condenser: Dispersed microbubble mediation of additional heat transfer in aqueous solutions due to phase change dynamics in airlift vessels. *Chemical Engineering Science*. 238: 116618, 2021.

[12] N. Abdulrazzaq, B. Al-Sabbagh, J.M.Rees, W. B. Zimmerman, "Purification of Bioethanol Using Microbubbles Generated by Fluidic Oscillation: A Dynamical Evaporation Model", Industrial & Engineering Chemistry Research 55:12909-12918, 2016.

[13] Al-yaqoobi A., Hogg D., Zimmerman W.B., Microbubble distillation for ethanol-water separation Int. J. Chem. Eng. 2016 1-10.

[14] R. B. Bird, W. E. Stewart, E. N. Lightfoot, *Transport Phenomena*, Wiley, 2007.

[15] S. Brittle, P. Desai, W. C. Ng, A. Dunbar, R. Howell, V. Tesař and W. B. Zimmerman, Minimising microbubble size through oscillation frequency control. *Chemical Engineering Research and Design*, 2015, **104**, 357-366.

[16] F. Rehman, G.Medley, H.C.H.Bandalusena , W.B. Zimmerman, Fluidic oscillator-mediated microbubble generation to provide cost effective mass transfer and mixing efficiency to the wastewater treatment plants. *Environmental Research*, 2015, **137**, 32-39.

[17] J. Hanotu, H. C. Bandulasena and W. B. Zimmerman, Microflotation performance for algal separation. *Biotechnol Bioeng*, 2012, **109**, 1663-1673.

[18] V. Tesař, Mechanisms of fluidic microbubble generation part II: Suppressing the conjunctions. *Chemical Engineering Science*, DOI: http://dx.doi.org/10.1016/j.ces.2014.04.021.

[19] V. Tesař, C.-H. Hung and W. B. Zimmerman, No-moving-part hybrid-synthetic jet actuator. *Sensors and Actuators A: Physical*, 2006, **125**, 159-169.

[20] V. Tesař. W.B. Zimmerman, S.Butler, H.C. H. Bandulasena, Microbubble generation. *Recent Patents on Engineering*, 2008, **2**, 1-8.

[21] P. Desai, M. Hines, Y. Riaz and W.B Zimmerman, Resonant pulsing frequency effect for much smaller bubble formation with fluidic oscillation. *Energies*, 2018, 11, 2680.

[22] P. D. Desai, W. C. Ng, M. J. Hines, Y. Riaz, V. Tesar and W. B. Zimmerman, Comparison of bubble size distributions inferred from acoustic, optical visualisation, and laser diffraction. *Colloids and Interfaces*, 2019, 3, 65.

[23] Animal and Plant Health Agency, 2007. Standard Methods for the Examination of Water and Wastewater - Part 4000 (Inorganic nonmetallic constituents), Section 4500-NH3. *In:* Animal and Plant Health Agency, G. U. (ed.). GOV.UK: APHA, 178.

[24] S. K. Marttinen, R. H. Kettunen, K. M. Sormunen, R. M. Soimasuo and J. A. Rintala, Screening of physical-chemical methods for removal of organic material, nitrogen, and toxicity from low strength landfill leachates. *Chemosphere*, 2002, **46**, 851-858.

[25] A. C. Silva, M. Dezotti and G. L. Sant'Anna Jr, Treatment and detoxification of a sanitary landfill leachate. *Chemosphere*, 2004, **55**, 207-214.

[26] C. Collivignarelli, G. Bertanza, M. Baldi and F. Avezzù, Ammonia stripping from MSW landfill leachate in bubble reactors: process modeling and optimization. *Waste Management & Research*, 1998, **16**, 455-466.

[27] L. M. Chu, M.H.Wong, and K. C. Cheung. Variations in the Chemical Properties of Landfill Leachate. *Water, Air, and Soil Pollution*, 1995, **94**, 209-221.

[28] K. C. Cheung, L. M. Chu and M. H. Wong, Ammonia stripping as a pretreatment for landfill leachate. *Water, Air, and Soil Pollution*, 1997, **94**, 209-221.

[29] E. G. Srinath and R. C. Loehr, Ammonia Desorption by Diffused Aeration. *Journal (Water Pollution Control Federation)*, 1974, **46**, 1939-1957.

[30] S. Guštin and R. Marinšek-Logar, Effect of pH, temperature and air flow rate on the continuous ammonia stripping of the anaerobic digestion effluent. *Process Safety and Environmental Protection*, 2011, 89, 61-66.

[31] S. Xu , L. Hoshan, R.Jiang, B. Gupta, E. Brodean , K. O'Neill, T. C. Seamans , J. Bowers , H. Chen, A practical approach in bioreactor scale-up and process transfer using a combination of constant P/V and vvm as the criterion, Biotechnol. Prog. 33(4):1146-1159, 2017.

[32] P. G. Smith and F. K. Arab, The role of air bubbles in the desorption of ammonia from landfill leachates in high pH aerated lagoon. *Water, Air, and Soil Pollution*, 1988, **38**, 333-343.

[33] S. N. Behera, M. Sharma, V. P. Aneja and R. Balasubramanian, Ammonia in the Atmosphere: A Review on Emission Sources, Atmospheric Chemistry and Deposition on Terrestrial Bodies, *Environ Sci Pollut Res Int*, 2013, 20, 8092-8131.

[34] T. de Donder and P. Van Rysselberghe, *Thermodynamic Theory of Affinity*, Stanford University Press, 1936.

[35] I. Prigogine, *From Being to Becoming Time and Complexity in the Physical Sciences /Ilya Prigogine*, W.H. Freeman, C1980, 1980.

[36] D. R. Stull, Vapor Pressure of Pure Substances—Correction. *Industrial & Engineering Chemistry*, 1947, 39, 1684-1684.

[37] F. Monlau, C. Sambusiti, E. Ficara, A. Aboulkas, A. Barakat and H. Carrère, New opportunities for agricultural digestate valorization: current situation and perspectives. *Energy Environ. Sci.*, 2015, **8**, 2600-2621.

[38] D. Frascari, F. Bronzini, G. Giordano, G. Tedioli and M. Nocentini, Long-term characterization, lagoon treatment and migration potential of landfill leachate: a case study in an active Italian landfill. *Chemosphere*, 2004, **54**, 335-343.

[39] T. Maehlum, Treatment of landfill leachate in on-site lagoons and constructed wetlands. *Wat. Sci. Tech.*, 1995, **32**, 129-135.

[40] M. X. Loukidou and A. I. Zouboulis, Comparison of two biological treatment processes using attached-growth biomass for sanitary landfill leachate treatment. *Environmental Pollution*, 2001, **111**, 273-281.

[41] A. Uygur and F. Kargi, Biological nutrient removal from pre-treated landfill leachate in a sequencing batch reactor. *Journal of Environmental Management*, 2004, 71, 9-14.

[42] J. Bae, S. Kim and H. Chang, Treatment of landfill leachates: ammonia removal via nitrification and denitrification and further COD reduction via Fenton's treatment followed by activated sludge. *Water Science and Technology*, 1997, **36**, 341-348.

[43] J. P. Y. Jokela, R. H. Kettunen, K. M. Sormunen and J. A. Rintala, Biological nitrogen removal from municipal landfill leachate: low-cost nitrification in biofilters and laboratory scale in-situ denitrification. *Water Research*, 2002, **36**, 4074087.

[44] H. D. Robinson and G. Grantham, The treatment of landfill leachates in on-site aerated lagoon plants: experience in Britain and Ireleand. *Water Research*, 1988, **22**, 733-747.

[45] C. D. Martin and K. D. Johnson, The use of extended aeration and in-series surface-flow welands for landfill leachate treatment. *Water Science and Technology*, 1995, **32**, 119-128.

[46] D. Trebouet, J. P. Schlumpf, P. Jaouen, J. P. Maleriat and F. Quemeneur, Effect of Operating Conditions on the Nanofiltration of Landfill Leachates: Pilot-Scale Studies. *Environmental Technology*, 1999, **20**, 587-596.

[47] D. Trebouet, J. P. Schlumpf, P. Jaouen and F. Quemeneur, Stabilized landfill leachate treatment by combined physicochemical–nanofiltration processes. *Water Research*, 2001, **35**, 2935-2942.

[48] I. Ozturk, M. Altinbas, I. Koyuncu, O. Arikan and C. Gomec-Yangin, Advanced physico-chemical treatment experiences on young municipal landfill leachates. *Waste Management*, 2003, **23**, 441-446.

[49] I. Kabdasli, Í. Öztürk, O. Tünay, S. Yilmaz and O. Arikan, Ammonia removal from young landfill leachate by magnesium ammonium phosphate precipitation and air stripping. *Water Science and Technology*, 2000, **41**, 237-240.

[50] T. Zhang, L. Ding and H. Ren, Pretreatment of ammonium removal from landfill leachate by chemical precipitation. *Journal of Hazardous Materials*, 2009, **166**, 911-915.

[51] X. Z. Li, Q. L. Zhao and X. D. Hao, Ammonium removal from landfill leachate by chemical precipitation. *Waste Management*, 1999, **19**, 409-415.

[52] F. Kargi and M. Y. Pamukoglu, Adsorbent supplemented biological treatment of pre-treated landfill leachate by fed-batch operation. *Bioresource Technology*, 2004, **94**, 285-291.

[53] F. Kargi and M. Yunus Pamukoglu, Simultaneous adsorption and biological treatment of pre-treated landfill leachate by fed-batch operation. *Process Biochemistry*, 2003, **38**, 1413-1420.

[54] N. Aghamohammadi, H. B. A. Aziz, M. H. Isa and A. A. Zinatizadeh, Powdered activated carbon augmented activated sludge process for treatment of semi-aerobic landfill leachate using response surface methodology. *Bioresource Technology*, 2007, **98**, 3570-3578.

[55] S. Liu, Q. Wang, X. Zhai, Q. Huang and P. Huang, Improved Pretreatment (Coagulation-Floatation and Ozonation) of Younger Landfill Leachate by Microbubbles. *Water Environment Research*, 2010, 82, 657-665.

[56] P. B. Moraes and R. Bertazzoli, Electrodegradation of landfill leachate in a flow electrochemical reactor. *Chemosphere*, 2005, **58**, 41-46.

[57] B. Liu, X. Y. Peng, Q. Tian and H. Zhao, Removal of Ammonia Nitrogen from Landfill Leachate by Ultrasound/Ultraviolet Process. *Applied Mechanics and Materials*, 2014, **448-453**, 536-539.

[58] S. Wang, X. Wu, Y. Wang, Q. Li and M. Tao, Removal of organic matter and ammonia nitrogen from landfill leachate by ultrasound. *Ultrasonics Sonochemistry*, 2008, **15**, 933-937.

[59] V. J. P. Vilar, E. M. R. Rocha, F. S. Mota, A. Fonseca, I. Saraiva and R. A. R. Boaventura, Treatment of a sanitary landfill leachate using combined solar photo-Fenton and biological immobilized biomass reactor at a pilot scale. *Water Research*, 2011, **45**, 2647-2658.

[60] A. Ž. Gotvajn, T. Tišler and J. Zagorc-Končan, Comparison of different treatment strategies for industrial landfill leachate. *Journal of Hazardous Materials*, 2009, **162**, 1446-1456.

[61] A. Cabeza, A. Urtiaga, M.-J. Rivero and I. Ortiz, Ammonium removal from landfill leachate by anodic oxidation. *Journal of Hazardous Materials*, 2007, **144**, 715-719.

[62] A. G. Vlyssides, P. K. Karlis, N. Rori and A. A. Zorpas, Electrochemical Treatment in Relation to pH of Domestic Wastewater Using Ti/Pt Electrodes. *Journal of Hazardous Materials*, 2002, 95, 215-226.

[63] A. Vlyssides, P. Karlis, M. Loizidou, A. Zorpas and D. Arapoglou, Treatment of Leachate from a Domestic Solid Waste Sanitary Landfill by an Electrolysis System. *Environmental Technology*, 2001, **22**, 1467-1476.

[64] L.-C. Chiang, J.-E. Chang and T.-C. Wen, Indirect oxidation effect in electrochemical oxidation treatment of landfill leachate. *Water Research*, 1995, **29**, 671-678.

Supplementary Data

Summary of the performances of the leachate treatment methods discussed.

These different methods have been adapted from various publications. The physico-chemical methods have been placed in Figure 10. The effectiveness of the method depends on the method in terms of treatment efficiency, operational parameters (operating costs, treatment time, whether ammonia is recovered/utilised/destroyed), and what is left for the remnant liquid.

Creating the leachate treatment performance matrix

Each of the sources were calculated a performance score based on the respective processing time to achieve a removal efficiency. The times and efficiencies were normalised to a scale of between 0-1 (0 being worst and vice-versa) which was done using the following equations:

$$\text{score(time)} = \frac{\max \text{time required out of all methods (h)} - \text{time for a particular treatment method (h)}}{\max \text{time required out of all methods (h)}}$$

$$\text{score(efficiency)} = \frac{\text{efficiency for a particular treatment method (\%)} - \min \text{eff achieved out of all methods (\%)}}{100\% - \min \text{eff achieved out of all methods (\%)}}$$

Take the equation for scoring the time performances: the maximum time recorded by any of the reviewed literature was 768 hours [38]. If the time for a particular method took 24 hours (e.g. stripping), then the performance factor/score would be (768-24)/768 = 0.9688. Qualitatively, this means that the stripping process is significantly more effective in terms of time than the lagooning method. On the other hand, if a process took 500 hours to completion, a score of 0.3490 would be calculated meaning that the process is only slightly more effective. This same rationale is used for the efficiency scoring.

The scores on their own do not give true indication as to performance however. A process may achieve 100% removal but take an infinite amount of time to complete and is therefore ineffective, hence why the scores must be combined. Using 'AND' Boolean logic combines the two scores by multiplication. It

follows that both score A AND score B must be effective to make a process effective overall. OR logic would not be suitable as, returning to the previous example, a process could still achieve a 50% effectiveness score for 100% removal over an infinite amount of time.

Clearly, there are some processes which will score lowly such as biological processes which require long processing times but they make up for this with low CAPEX and OPEX. This method is crude but suitable for analysing a broad range of processes with an even broader set of variables and limited costing data. Table 3 lists the different treatment methods used in literature.

Table 4 defines what the performance terminology is in terms of effectiveness.

Finally, the scores are categorised into groups based on Table 5.

Table 3 Performance versus treatment method as discussed in the literature

	Performance			
	Not effective	**Somewhat effective**	**Effective**	**Highly effective**
Biological treatment	Maehlum [39] Loukidou and Zouboulis [40] Uygur and Kargi [41]		Bae et al. [42] Jokela et al. [43]	
Lagooning	Frascari et al. [38]		Robinson and Grantham [44] Martin and Johnson [45]	

		Performance			
		Not effective	**Somewhat effective**	**Effective**	**Highly effective**
Nanofiltration		Marttinen et al [24] Trebouet et al. [46]. Trebouet et al. [47]	Marttinen et al [24]		
Physico-chemical methods	**Chemical precipitation**			Ozturk et al. [48] Kabdasli et al. [49] Zhang et al. [50]	Li et al. [51]
	Adsorption	Kargi and Pamukoglu [52] Kargi and Pamukoglu [53]	Uygur and Kargi [41]	Aghamohammadi et al. [54]	

		Performance			
		Not effective	**Somewhat effective**	**Effective**	**Highly effective**
	Oxidation	Liu et al. [55]	Moraes and Bertazzoli [56]	Liu et al. [55], [57] Vlyssides et al. [62]	Wang et al. [58] Liu et al. [57] Vilar et al. [59] Gotvajn et al. [60] Cabeza et al. [61] Vlyssides et al. [63] Chiang et al. [64]
	Stripping		Marttinen et al. [24] Collivignarelli et al. [26]	Cheung et al. [28] Kabdasli et al. [49] Marttinen et al. [24] Silva [88] et al. [25]	**RESEARCH OPPORTUNITY**

Table 4 Categorisation of leachate treatment methods based on scores.

Adjective(s)	**Score rating**
Not effective	0-0.4
Somewhat effective	0.4-0.6
Effective	0.6-0.9
Highly effective	0.9-1.0

Table 5 Performance scores for the leachate treatment processes.

	Reference	**Processing time (h)**	**Processing time score**	**Removal efficiency (%)**	**Removal efficiency score**	**Final score**
Oxidation	Liu et al. [55]	1	0.9987	10	0.00	0.00
	Liu et al. [55]	1	0.9987	66	0.62	0.62
	Wang et al. [58]	1.5	0.9980	96	0.96	0.95
	Liu et al. [57]	6	0.9922	98.5	0.98	0.98
	Vilar et al. [59]	3	0.9961	100	1.00	1.00
	Gotvajn et al. [60]	0.5	0.9993	93	0.92	0.92
	Cabeza et al. [61]	6	0.9922	100	1.00	0.99

	Reference	Processing time (h)	Processing time score	Removal efficiency (%)	Removal efficiency score	Final score
Stripping	Vlyssides et al. [62]	2	0.9974	72	0.69	0.69
	Moraes and Bertazzoli [56]	3	0.9961	49	0.43	0.43
	Vlyssides et al. [63]	1	0.9987	100	1.00	1.00
	Chiang et al. [64]	4	0.9948	100	1.00	0.99
		24	0.9688	70	0.67	0.65
		24	0.9688	81	0.79	0.76
	Cheung et al. [28]	24	0.9688	90	0.89	0.86
	Kabdasli et al. [49]	24	0.9688	85	0.83	0.81
	Marttinen et al [24]	24	0.9688	89	0.88	0.85
		96	0.8750	64	0.60	0.53
	Silva et al. [25]	96	0.8750	99	0.99	0.87
Adsorption	Collivignarelli et al. [26]	8	0.9896	50	0.44	0.44
		30	0.9609	28	0.20	0.19

	Reference	Processing time (h)	Processing time score	Removal efficiency (%)	Removal efficiency score	Final score
Chemical precipitation	Kargi and Pamukoglu [52]	30	0.9609	16	0.07	0.06
	Uygur and Kargi [41]	21	0.9727	44	0.38	0.37
	Kargi and Pamukoglu [53]	30	0.9609	16	0.07	0.06
	Aghamohammadi et al [54]	53	0.9310	69	0.66	0.61
	Li et al. [51]	0.25	0.9997	98	0.98	0.98
	Ozturk et al. [48].	1	0.9987	85	0.83	0.83
	Kabdasli et al. [49]	168	0.7813	97	0.97	0.76
	Zhang et al. [50]	1	0.9987	85.5	0.84	0.84
Nanofiltration	Marttinen et al. [24]	9	0.9883	27	0.19	0.19
	Marttinen et al. [24]	9	0.9883	50	0.44	0.44
		9	0.9883			
	Trebouet et al. [46]	240	0.6875	13	0.03	0.02

	Reference	Processing time (h)	Processing time score	Removal efficiency (%)	Removal efficiency score	Final score
Lagooning	Trebouet et al. [46]	240	0.6875	21.2	0.12	0.09
	Trebouet et al. [47]	12	0.9844	12	0.02	0.02
	Trebouet et al. [47]	12	0.9844	21	0.12	0.12
	Frascari et al. [38]	768	0.0000	77	0.74	0.00
	Robinson and Grantham [44]	240	0.6875	99.5	0.99	0.68
	Maehlum [39]		1.0000			
Biological processes	Martin and Johnson [45]	480	0.3750	90	0.89	0.33
	Bae et al [42]	30	0.9609	87.5	0.86	0.83
	Lo (1996)	720	0.0625	99	0.99	0.06
	Maehlum [39]		1.0000			
	Loukidou and Zouboulis [40]	528	0.3125	85	0.83	0.26
	Jokela et al [43]	120	0.8438	90	0.89	0.75
	Bae et al [42]			87.5	0.86	

	Reference	Processing time (h)	Processing time score	Removal efficiency (%)	Removal efficiency score	Final score
	Uygur and Kargi [41]	21	0.9727	31	0.23	0.23